NMR identification of local structural preferences in HIV-1 protease tethered heterodimer in 6 M guanidine hydrochloride

Neel S. Bhavesh[a], Sanjay C. Panchal[a], Rohit Mittal[b], Ramakrishna V. Hosur[a,*]

[a] *Department of Chemical Sciences, Tata Institute of Fundamental Research, Homi Bhabha Road, Mumbai 400 005, India*
[b] *Department of Biological Sciences, Tata Institute of Fundamental Research, Homi Bhabha Road, Mumbai 400 005, India*

Received 24 September 2001; accepted 26 September 2001

First published online 21 November 2001

Edited by Thomas L. James

Abstract Understanding protein folding requires complete characterization of all the states of the protein present along the folding pathways. For this purpose nuclear magnetic resonance (NMR) has proved to be a very powerful technique because of the great detail it can unravel regarding the structure and dynamics of protein molecules. We report here NMR identification of local structural preferences in human immunodeficiency virus-1 protease in the 'unfolded state'. Analyses of the chemical shifts revealed the presence of local structural preferences many of which are native-like, and there are also some non-native structural elements. Three-bond H^N–H^α coupling constants that could be measured for some of the N-terminal and C-terminal residues are consistent with the native-like β-structure. Unusually shifted ^{15}N and amide proton chemical shifts of residues adjacent to some prolines and tryptophans also indicate the presence of some structural elements. These conclusions are supported by amide proton temperature coefficients and nuclear Overhauser enhancement data. The locations of the residues exhibiting preferred structural propensities on the crystal structure of the protein, give useful insights into the folding mechanism of this protein. © 2001 Published by Elsevier Science B.V. on behalf of the Federation of European Biochemical Societies.

Key words: Human immunodeficiency virus-1 protease; Denatured/unfolded protein; Guanidine hydrochloride; Backbone resonance assignment; Nuclear magnetic resonance; HNN; HN(C)N; Residual structural propensity

1. Introduction

The ability of a polypeptide chain to fold fast to its native state has given rise to a very important interdisciplinary problem of the current time, namely, the 'protein-folding problem'. The key to solving the protein-folding problem lies in an accurate structural and dynamic characterization of all the species along the folding pathways, including the native, the partially folded intermediates and the fully denatured states. X-ray crystallography and nuclear magnetic resonance (NMR) spectroscopy have been extensively used for structure determination of folded proteins but fully denatured proteins have evaded detailed structural investigation because of their heterogeneity and conformational flexibility. The primary difficulty from the NMR point of view has been the poor chemical shift dispersions which hamper resonance assignments. Nonetheless, relatively better spectral dispersion of ^{15}N and $^{13}C'$ resonances have been used by many authors to get resonance assignments in several unfolded proteins [1–13].

For proteins which fold readily to stable native states, the unfolded states will have to be created by use of different denaturing agents such as urea, guanidine hydrochloride, extreme pH conditions, etc. For many small proteins, there is strong evidence for a close structural correspondence between equilibrium partly unfolded states, created as above, and kinetic intermediates during the folding process [14–17]. In such cases, a systematic following of the residual structures as a function of the perturbations taking the protein from fully denatured state to the native state, allows stepwise monitoring of the folding process. Under extreme conditions, the observed residual structures represent local preferences and suggest initial folding events during a folding reaction. In several proteins native-like and/or non-native-like residual secondary structures have been observed under such extreme denaturing conditions [1,2,8,11,12,18,19].

Human immunodeficiency virus (HIV)-1 protease is an aspartyl protease that catalyzes the cleavage of several polypeptides yielding mature proteins that are required for the function of the acquired immunodeficiency syndrome (AIDS) virus [20–21]. The functional protease is a 22 kDa homodimer that self-assembles from two identical polypeptide chains of 99 residues each. Extensive NMR structural and dynamic studies have been reported on the folded protein, complexed to different inhibitors [22–26]. However, to date, there have been no reports on the unfolded state of the protein. Thus the present study focuses on the 'unfolded' state of a tethered dimer (TD) construct of the protease, wherein, the C-terminal of one monomer is covalently joined to the N-terminal of another monomer by a GGSSG linker [27–28] resulting in a single polypeptide chain of 203 amino acid residues. The chain also carries two point mutations, C95M in the first half and C195A in the second half. Complete backbone assignments have been obtained for the denatured protein (in 6 M guanidine hydrochloride). The carbon chemical shifts, the H^NH^α coupling constants and the nuclear Overhauser effects (NOEs) indicate the presence of some structural preferences. The locations of these residues at the dimer interface and the hydrophobic nature of the residues suggest that hydrophobic clustering could be an initial folding event of the functional protein.

*Corresponding author. Fax: (91)-22-215 2110.
E-mail address: hosur@tifr.res.in (R.V. Hosur).

Abbreviations: NMR, nuclear magnetic resonance; HIV, human immunodeficiency virus; AIDS, acquired immunodeficiency syndrome; HSQC, heteronuclear single quantum coherence; TROSY, transverse relaxation-optimized spectroscopy

0014-5793/01/$20.00 © 2001 Published by Elsevier Science B.V. on behalf of the Federation of European Biochemical Societies.
PII: S0014-5793(01)03066-6

2. Materials and methods

2.1. Protein preparation

HIV-1 protease TD cloned in pET 11a expression vector was obtained as a kind gift from Dr. M.V. Hosur, Bhabha Atomic Research Centre, Mumbai, India. This clone carried C95M mutation in one of the monomers. To avoid oxidation of the cysteine residue at the dimerization domain during long three-dimensional (3D) experiments, we mutated cysteine 95 in the other monomer (C195) to alanine. This C195A mutation was achieved using standard polymerase chain reaction techniques. The mutated gene was cloned back into pET 11a expression vector and expressed in *Escherichia coli* BL21 (*DE3*) cells.

2.2. NMR sample

^{15}N-Labeled and ^{13}C,^{15}N-labeled HIV-1 protease mutant (C95M, C195A) TD was produced by overexpression in minimal media and purified using the procedure described elsewhere [26]. For NMR sample preparation, the protein was concentrated to $\sim$1 mM and exchanged with pH 5.2 NMR buffer consisting of 50 mM Na-acetate, 5 mM EDTA, 150 mM DTT and 6 M guanidine hydrochloride, by ultrafiltration.

2.3. NMR data acquisition and processing

NMR spectra were recorded at ^{1}H Larmor frequency of 600.052 MHz using a three-channel Varian Unity+ spectrometer equipped with pulsed field gradients. All spectra were recorded at 32°C. NMR spectra recorded and the parameters used are listed in Table 1.

For the triple resonance experiments used for resonance assignments, the ^{1}H and ^{15}N carrier frequencies were set at 4.71 ppm (water) and 119 ppm, respectively. The ^{13}C carrier frequency was set at 56.0 ppm for HNN [29], HN(C)N [29], HNCA [30], HN(CO)CA [31], 45.0 ppm for CBCANH [32], CBCA(CO)NH [33] and 174.0 ppm for HNCO [30], respectively. Prior to Fourier transformation and zero-filling, data were apodized with a sine-squared weighting function shifted by 60° in all dimensions. For coupling constant estimations, a high resolution transverse relaxation-optimized spectroscopy (TROSY) [34] was recorded with 4096 (t_2)$\times$512 (t_1) complex time domain data matrix and the data was zero-filled to a matrix size of 16 384$\times$2048 complex points. The data was apodized by sine squared functions shifted by 20 and 30°, respectively, along the t_2 and t_1 dimensions. Temperature coefficients for amide protons were measured from a series of TROSY spectra recorded at 3°C intervals between 25 and 46°C. A 3D nuclear Overhauser enhancement spectroscopy (NOESY)-heteronuclear single quantum coherence (HSQC) spectrum was recorded with 96 (t_1), 48 (t_2) and 1024 (t_3) time domain points. The data were apodized with a sine-squared weighting function shifted by 60° in all dimensions. After zero filling and Fourier transformation the final matrix had 1024, 256 and 256 points along the F_3, F_2 and F_1 dimensions, respectively. Processing of spectra was carried out using *Felix 97* software (Molecular Simulations, San Diego, CA, USA). In all spectra, ^{1}H, ^{13}C and ^{15}N chemical shifts were, respectively, referenced to HDO (4.71 ppm at 32°C), indirectly to 2,2-dimethyl-2-silapentane-5-sulfonic acid, and to trimethylsilyl sodium propionate.

3. Results and discussion

3.1. Backbone resonance assignments

The traditional method of sequential assignment by standard triple resonance 3D methods (HNCA, HN(CO)CA, CBCANH and CBCA(CO)NH) relies mainly on $^{13}C^{\alpha}$, $^{13}C^{\beta}$, $^{1}H^{\alpha}$, $^{1}H^{\beta}$ and H^{N} resonances and is used routinely when resonance dispersion is very good. However, when these resonances are poorly dispersed, which is the case in denatured proteins, the standard methods have limited success. Fortunately, however, the residual chemical shift dispersion of ^{15}N is still large and experiments exploiting these dispersions are likely to be more useful. In this context, we recently described two new 3D triple resonance experiments, HNN, HN(C)N, which correlate H^{N} and ^{15}N resonances sequentially along the polypeptide chain of a doubly (^{13}C,^{15}N) labeled protein ([29] and references therein). Using these HNN and HN(C)N spectra we could obtain complete ^{15}N and H^{N} resonance assignments for all non-proline residues in the HIV-TD protein. An illustrative stretch of sequential connectivities is shown in Fig. 1 and all the assignments are displayed in the TROSY spectrum in Fig. 2. For residues P1, Q2, V3, T4, G94, T96, L97 and N98 two sets of peaks are seen due to the asymmetry introduced by the linker and the point mutations. Of these, N198, N98, L197, L97, T196, T96 and G194, G94 have been domain specifically assigned. Subsequent to these ^{15}N and amide proton assignments, complete $^{13}C^{\alpha}$, $^{13}C^{\beta}$ and $^{13}C'$ resonance assignments were obtained for all residues using the standard HNCA HN(CO)CA, CBCANH, CBCA(CO)NH and HNCO spectra. All the assignments have been deposited in the BioMagResBank under the accession number 5062.

3.2. Analysis of chemical shifts and residual structures

^{13}C chemical shifts of C′, C^{α} and C^{β} are useful indicators of secondary structure in folded proteins [35–38]. In order to detect the presence of residual structures in the unfolded protein, under the strong denaturing condition used, chemical shift deviations from random coil values for $^{13}C^{\alpha}$, $^{13}C^{\beta}$ and $^{13}C'$ resonances have to be calculated. However, there are more than one set of random coil values published in the literature and these differ because of the experimental conditions used in arriving at those values. Wishart et al. [39] used 1 M urea, pH 5 and 25°C for their experiments on the peptides chosen, whereas Schwarzinger et al. [40,41] derived another set of values from peptide spectra recorded in 8 M urea, pH 2.3 and 20°C so as to obtain a better data set for their apomyoglobin protein. Schwarzinger et al. also observed that

Table 1
NMR experiments and their parameters

Experiment	Time domain complex points			Spectral width (Hz)			Matrix size	nt	Time (h)
	t_1	t_2	t_3	SW1	SW2	SW3			
^{15}N TROSY	512 (N)	4096 (H)	–	2300	8500	–	16 384×2048	4	3.5
^{15}N HSQC-TOCSY	256 (N)	2048 (H)	–	2300	8500	–	4096×2048	64	14.0
HNN	68 (N)	68 (N)	1024 (H)	2300	2300	8500	256×256×1024	4	29.5
HN(C)N	68 (N)	68 (N)	1024 (H)	2300	2300	8500	256×256×1024	8	33.5
HNCA	100 (C)	68 (N)	1024 (H)	6000	2300	8500	256×256×1024	4	45.5
HN(CO)CA	100 (C)	68 (N)	1024 (H)	6000	2300	8500	256×256×1024	4	44.5
CBCANH	80 (C)	68 (N)	1024 (H)	13 500	2300	8500	256×256×1024	4	33.5
CBCA(CO)NH	80 (C)	68 (N)	1024 (H)	13 500	2300	8500	256×256×1024	4	34.0
HNCO	50 (C)	50 (N)	1024 (H)	2500	2300	8500	256×256×1024	8	31.0
^{15}N NOESY-HSQC	96 (H)	48 (N)	1024 (H)	8500	2300	8500	256×256×1024	4	31.0

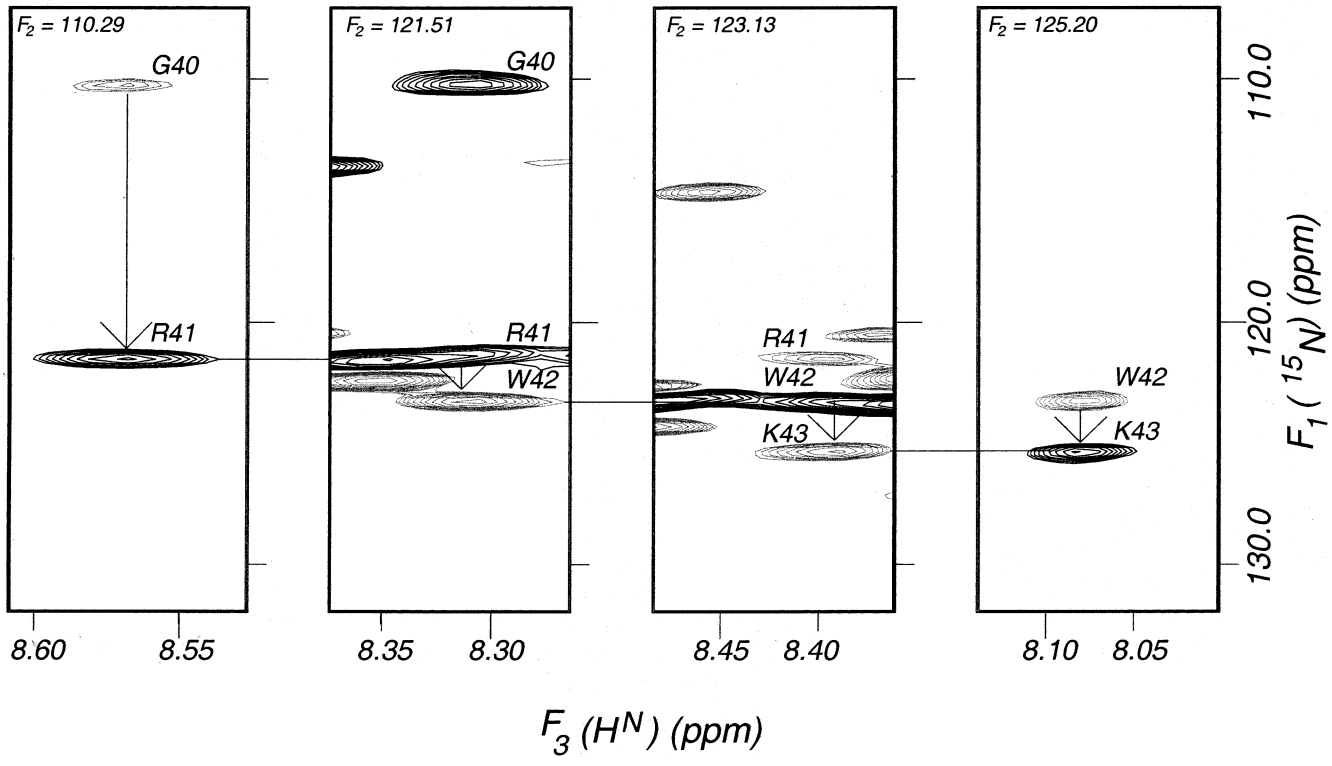

Fig. 1. Illustrative sequential ^{15}N connectivities in the HNN spectrum of HIV-TD protein. Appropriate strips at the correct H^N chemical shifts in the (F_1,F_3) planes have been taken. Both positive (thick) and negative (light) contours have been plotted.

corrections will have to be applied for sequence effects and provided a set of rules for these corrections. We analyzed our data using both the data sets and applied corrections as suggested by Schwarzinger et al. [41]. It was observed that C′ chemical shift deviations were very sensitive to the choice of the data set. This suggested that neither of the data sets would be suitable for C′, since the present data has been acquired in 6 M guanidine hydrochloride and not in urea. Thus C′ chemical shift deviations could not be used to derive structural information. The C^β chemical shifts also did not have much diagnostic value. On the other hand the C^α chemical shift deviations displayed similar patterns for either of the data sets, though the magnitudes differed slightly. The sequence-dependent correction did make a significant contribution in that many observed values calculated using the random coil values as given by Wishart et al. [39] then appeared close to the random coil values. This data is shown in Fig. 3.

There are interesting features in the chemical shift deviations shown above. First of all, although for a large number of residues the chemical shifts are close to random coil values, there are many residues for which the deviations are quite substantial. These deviations represent individual (ψ,ϕ) propensities, being negative for β structures and positive for α-structures. We notice that residues 1, 3, 5, 7 at the N-terminal, residues 21, 25 near the active site, residues 34, 37, 43, 44 near the loops, residues 53, 55, 56, in the flap area, residues 66, 69 on the outer surface, residues 79–84 around the active site and residues 197, 198 of the second half which participate in the β-sheet at the dimer interface exhibit high β-structure propensities. Likewise, residues 8, 10, 24, 40, 61, 63, 65, 67, 68, 88, 90 and 92 exhibit high α helical propensities. Referring to the native structural elements, also indicated in the figure, it is evident that the propensities at the N-terminal, the flap and the residues 88, 90, 92 are native-like and the rest are non-native. It is very interesting to note that the six prolines at positions 1, 9, 39, 44, 79, 81 have very significant influence on

Table 2
H^N–H^α coupling constants and amide proton temperature coefficients of selected residues in HIV-1 protease TD

Residue	$^3J(H^N–H^\alpha)$ (measured)	$^3J(H^N–H^\alpha)$ (random coil value) [48]	Temperature coefficients (ppb/K), $-d\delta/dT$
Q2	7.4	7.1	8.10
V3	7.8, 7.5	7.2	8.44, 9.48
T4	9.0, 8.8	7.9	9.40, 8.80
M95	7.2	7.1	7.60
T96	8.6	7.9	8.27
T196	9.0	7.9	8.43
L97	7.7	6.8	8.92
L197	7.5	6.8	9.56
N98	8.5	7.7	8.31
N198	7.6	7.7	8.06
F99	8.1	7.3	9.42

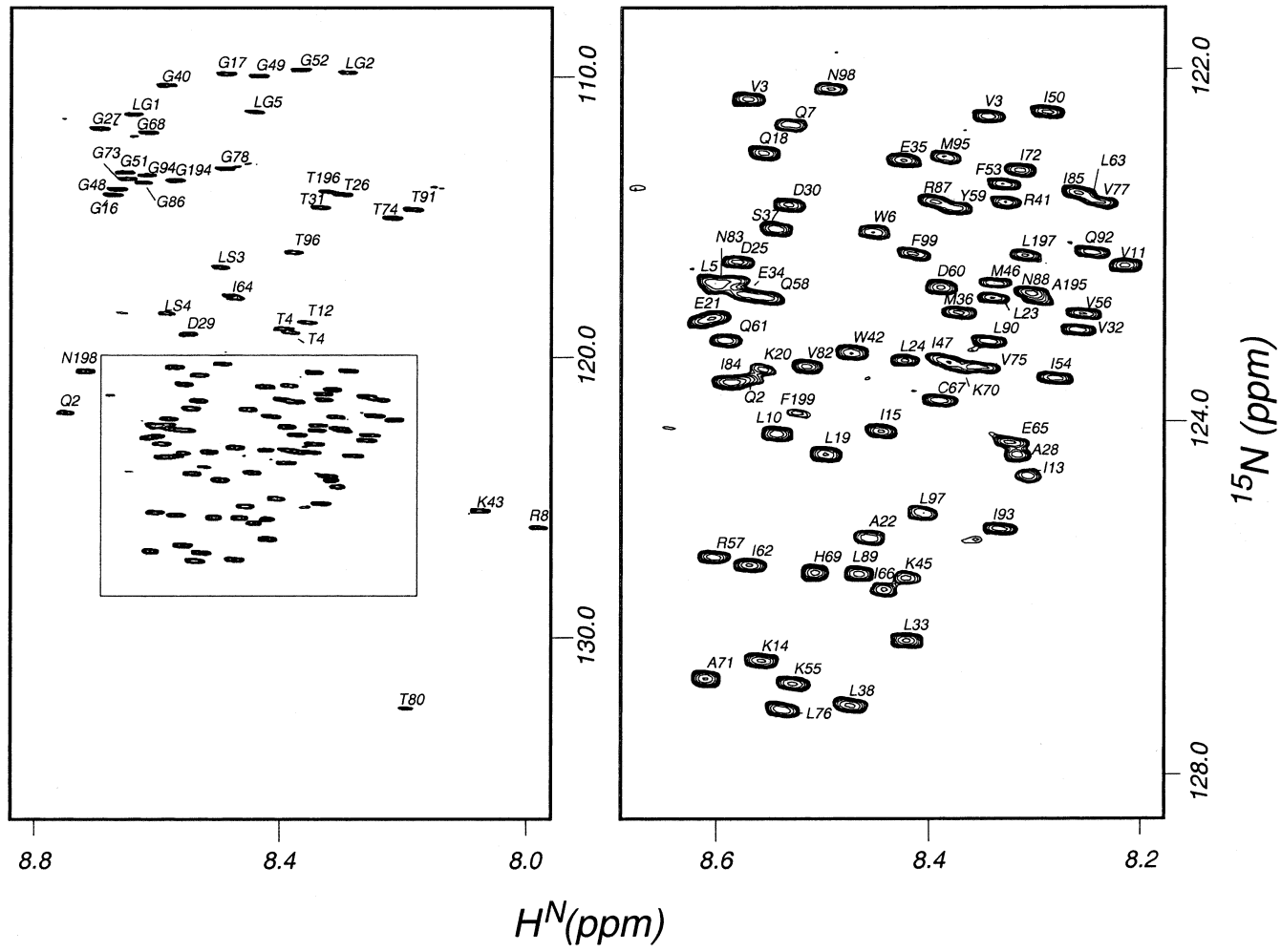

Fig. 2. ^{1}H–^{15}N TROSY spectrum of HIV-TD with sequence-specific assignments. The linker residues are labeled with a prefix L. G194, A195, T196, L197, N198 and F199 correspond to the residues in the second monomer of the TD. Rest of the residues in the two monomers are equivalent.

the structural propensities. Prolines at 9, 39, 79 have in fact forced non-native secondary structural propensities in the neighboring residues.

In addition to the above, some of the amide and ^{15}N chemical shifts also indicate the presence of some preferred structural propensities: (i) ^{15}N chemical shift of T80 is unusually downfield (132.30 ppm). (ii) Likewise, amide proton chemical shifts of lysine 43 and arginine 8 are quite upfield shifted. Both the residues have tryptophans as near neighbors. It is likely that K43 and R8 amides experience ring current effects from W42 and W6 tryptophans, respectively.

3.3. H^N–H^α coupling constants (J)

Three-bond H^N–H^α coupling constants provide valuable secondary structural information in folded proteins. β-Structures are characterized by large coupling constant values in the range 8–10 Hz, while α-helical structures are characterized by values in the range 3–5 Hz. In unfolded proteins, however, the heterogeneity and conformational averaging leads to average values of 6–7.5 Hz [19]. Nonetheless, values significantly different from these average random coil values would indicate definite propensities for the structures.

The most common method for measuring the H^N–H^α coupling constants relies on the HNHA experiment [42] or the

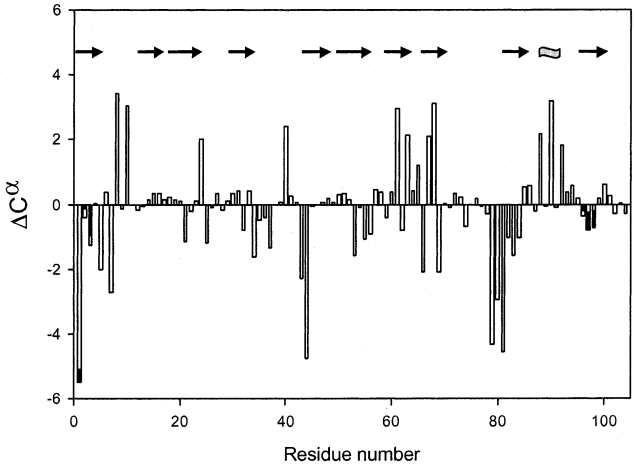

Fig. 3. Secondary chemical shifts, corrected for sequence-dependent contribution, for $^{13}C^\alpha$ resonances of HIV-TD in 6 M guanidine hydrochloride. A negative value in $\Delta^{13}C^\alpha$, is indicative of β-type backbone conformation [35–38] and a positive value is indicative of α-helical conformation. For interpretation of structural propensities we consider only those deviations which are larger than 0.7 ppm. The secondary structure elements in the folded protein (β-sheet by thick arrow and α-helix by shaded box) are also shown.

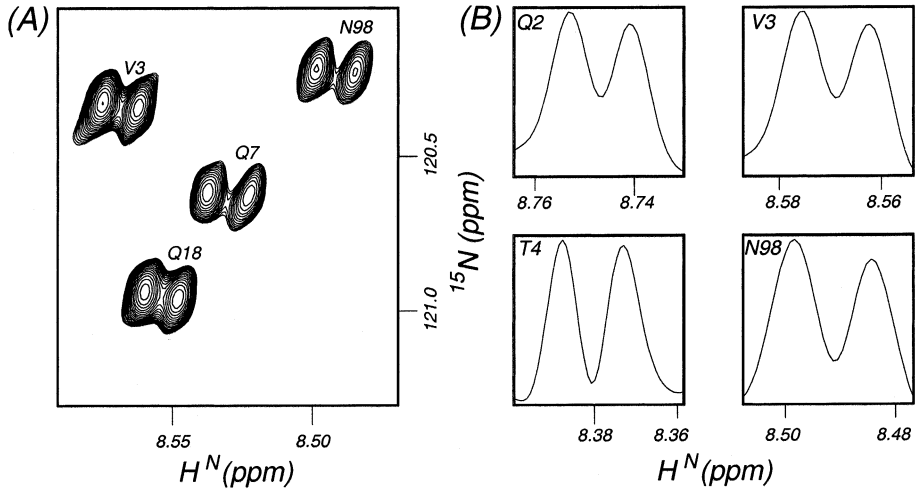

Fig. 4. A: A selected region from high resolution ^{1}H-^{15}N TROSY spectrum of HIV-TD showing the fine structures in the cross peaks. B: 1D cross-sections through a few cross peaks showing the H^{N}–H^{α} *J*-splitting.

HNCA-*J* experiment [43]. In the former the coupling constants are derived from the ratios of the diagonal to cross-peak intensities in the different ^{15}N planes of the 3D spectrum, and in the latter they are measured from peak multiplet structures. While these work well for folded proteins with well resolved peaks, they have serious problems for unfolded proteins where chemical shift dispersion is poor and reliable estimation of the peak intensities or separations is difficult. Relaxation losses also contribute to the uncertainties in intensity measurements in HNHA. Therefore we decided to measure these coupling constants from a high resolution TROSY spectrum itself, where this information is contained in the fine structure of the correlation peaks; it is surprising that, at least to our knowledge, this simple strategy has not been used in the literature. When we analyzed the fine structures in our spectra we discovered that for most residues, there were two sets of peaks with small chemical shift differences (comparable in magnitude to coupling constants) and this indicated a small non-equivalence between the two halves of the TD. For a few residues at the N-terminal and C-terminal, however, the two sets of peaks are very well separated (Fig. 2) and hence they could be analyzed unambiguously for the coupling constant values. Fig. 4 shows a few cross-peaks (A) and a few cross-sections (B) through some of the peaks. The measured *J* values for all the resolvable residues are listed in Table 2. It is interesting to note that the *J* values show a certain enhanced

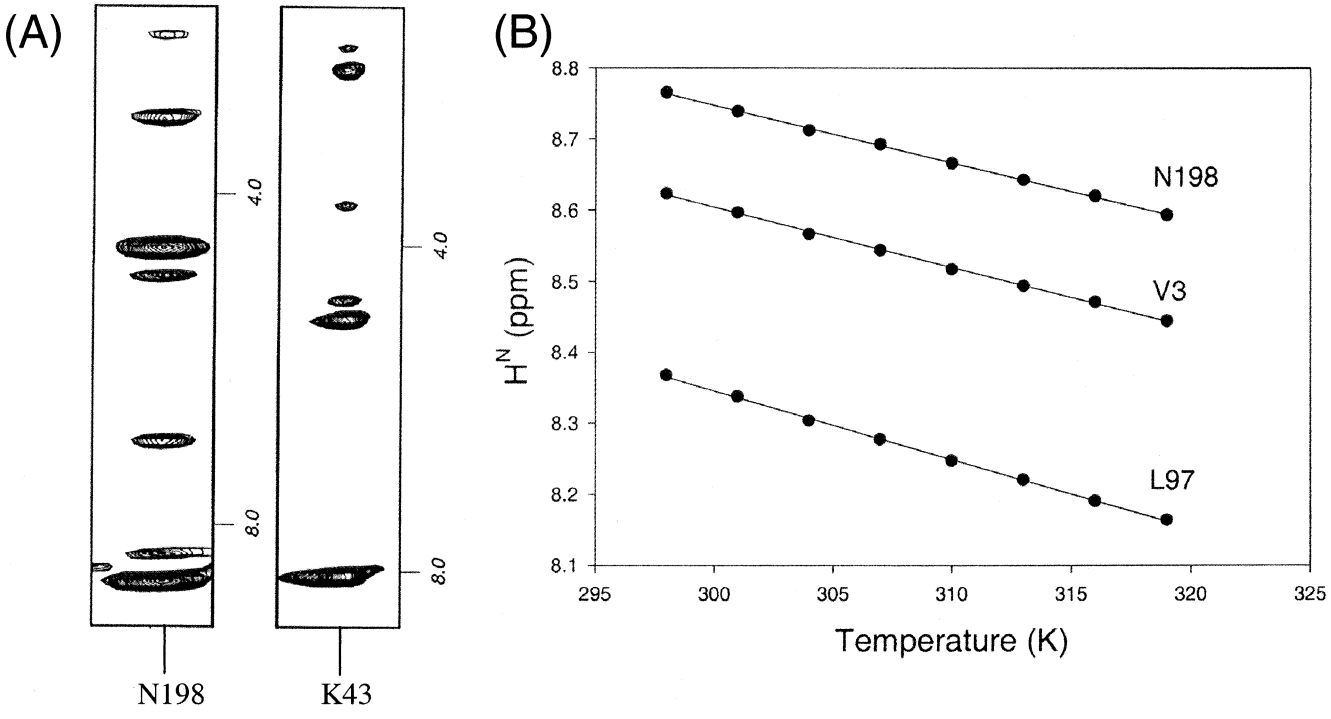

Fig. 5. A: Strips at the amide proton chemical shifts (F_3) of N198 and K43 residues from the ^{1}H–^{15}N NOESY-HSQC spectrum of HIV-TD in 6 M guanidine hydrochloride. Although no specific assignment of the NOEs is given, it is clear that some of the NOEs are intraresidue and others interresidue, in nature. B: Temperature dependence of a few amide protons and their linear fits to derive the temperature coefficients.

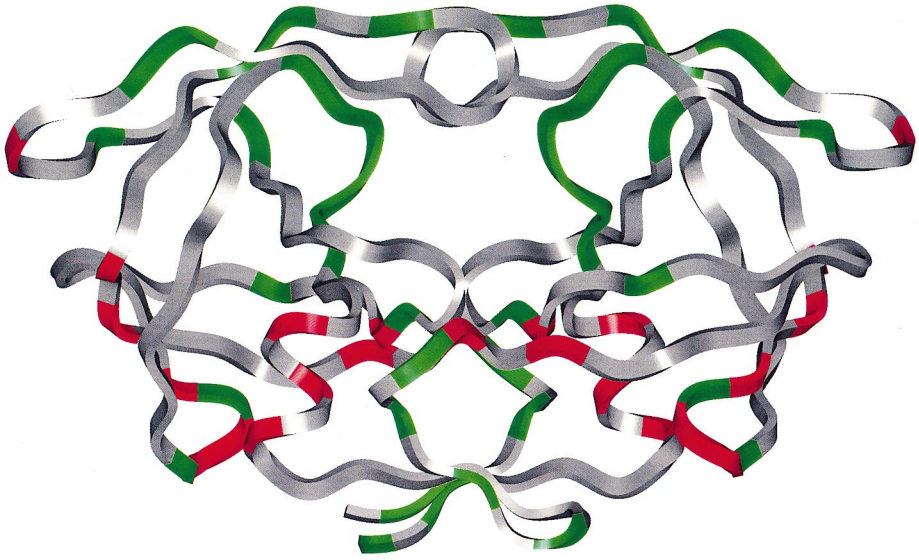

Fig. 6. The residual structural propensities derived from the NMR data are displayed on the crystal structure of HIV-1 protease TD [44]. Residues exhibiting high β-structure propensities are shown in green, while the residues exhibiting high α-helix propensities are shown in red.

propensity for β-structures for these residues, and this is consistent with the conclusions derived from the chemical shift analysis.

3.4. NOEs

The 3D NOESY-HSQC spectrum showed a number of NOEs from amide protons to α, β and other side chain protons. Although a large number of these could not be analyzed in a meaningful manner because of insufficient resolution in the spectra, the NOEs emanating from some of the amides distinctly seen in the HSQC spectra such as Q2, N198, K43, etc. could be readily followed. Fig. 5A shows strips belonging to the amides of K43 and N198. Clearly, a number of NOEs are seen, some of which would be intraresidue and others interresidue correlations, to α, β and other side chain protons. Considering that in the native folded protein, the N-terminal of first half and the C-terminal of the second half are engaged in a short β-sheet formation, the above observation supports the conclusion that the residues at the N- and C-terminal have a high propensity for the native-like β-structures. Furthermore, an important observation was the absence of any NOE from the amide of T80 which occurs at a distinct position in the HSQC spectrum. This suggests that the segment 79–84 which seemed like corresponding to a contiguous stretch of β-type residual secondary structure on the basis of chemical shift deviations, does not seem to be so on the basis of NOE data. The peptide in this region may be flexible, which may be the reason for the absence of NOEs. It remains a puzzle why the ^{15}N of T80 is so unusually downfield shifted.

3.5. Amide proton temperature coefficients

For the residues in the two halves of the dimer, which produced distinct peaks, we measured the amide proton temperature coefficients by recording TROSY spectra in the temperature in the range 25–46°C at 3° intervals. The chemical shift data were then analyzed by linear regression to estimate the slope and hence the temperature coefficients. A few illustrative fits are shown in Fig. 5B and all the measured temperature coefficients are listed in Table 2 along with the coupling constants. We observe that the temperature coefficients are mostly greater than 8 ppb/K which is the characteristic value for random coils [19]. This rules out the presence of any persistent secondary structure.

3.6. Implications for protein folding

Fig. 6 shows the locations of all the above local structural preferences on the crystal structure of the HIV-1 TD molecule (PDB ID: 1G6L) [44]. These indicate potential nucleation sites and possible initial structures during the folding of this protein. Of course, when folding is initiated by dilution to reduce the denaturant concentrations, different molecules can proceed along different potential energy channels (see reviews [45–47]) making and stabilizing different types of secondary and tertiary contacts. It is interesting to observe that much of the preferred structural propensity is in residues at the dimer interface and this includes the cavity at the active site. A large number of these residues are hydrophobic in nature suggesting that hydrophobic clustering may be a strong driving force for the initial folding events of the protein.

Acknowledgements: The facilities provided by the National Facility for High Field NMR, supported by the Government of India, are gratefully acknowledged. We thank Dr. M.V. Hosur of Bhabha Atomic Research Centre, Mumbai for the clone of the TD protein. N.S.B. thanks Mr. Ram K. Mishra, Department of Biological Sciences, Tata Institute of Fundamental Research, Mumbai for his help during site-directed mutagenesis.

References

[1] Neri, D., Wider, G. and Wuthrich, K. (1992) Science 257, 1559–1563.
[2] Logan, T.M., Theriault, Y. and Fesik, S.W. (1994) J. Mol. Biol. 236, 637–648.
[3] Arcus, V.L., Vuilleumier, S., Freund, S.M., Bycroft, M. and Fersht, A.R. (1994) Proc. Natl. Acad. Sci. USA 91, 9412–9416.
[4] Buck, M., Schwalbe, H. and Dobson, C.M. (1995) Biochemistry 34, 13219–13232.
[5] Frank, M.K., Clore, G.M. and Gronenborn, A.M. (1995) Protein Sci. 4, 2605–2610.

[6] Wong, K.B., Freund, S.M. and Fersht, A.R. (1996) J. Mol. Biol. 259, 805–818.
[7] Schwalbe, H., Fiebig, K.M., Buck, M., Jones, J.A., Grimshaw, S.B., Spencer, A., Glaser, S.J., Smith, L.J. and Dobson, C.M. (1997) Biochemistry 36, 8977–8991.
[8] Blanco, F.J., Serrano, L. and Forman-Kay, J.D. (1998) J. Mol. Biol. 284, 1153–1164.
[9] Penkett, C.J., Redfield, C., Jones, J.A., Dodd, I., Hubbard, J., Smith, R.A.J., Smith, L.J. and Dobson, C.M. (1998) Biochemistry 37, 17054–17067.
[10] Hennig, M., Bermel, W., Spencer, A., Dobson, C.M., Smith, L.J. and Schwalbe, H. (1999) J. Mol. Biol. 288, 705–723.
[11] Eliezer, D., Chung, J., Dyson, H.J. and Wright, P.E. (2000) Biochemistry 39, 2894–2901.
[12] Bai, Y., Chung, J., Dyson, H.J. and Wright, P.E. (2001) Protein Sci. 10, 1056–1066.
[13] Peti, W., Smith, L.J., Redfield, C. and Schwalbe, H. (2001) J. Biomol. NMR 19, 153–165.
[14] Jemmings, P.A. and Wright, P.E. (1993) Science 262, 892–896.
[15] Colon, W. and Roder, H. (1996) Nat. Struct. Biol. 3, 1019–1025.
[16] Raschke, T.M. and Marqusee, S. (1997) Nat. Struct. Biol. 4, 298–304.
[17] Hosszu, L.L., Craven, C.J., Parker, M.J., Lorch, M., Spencer, J., Clarke, A.R. and Waltho, J.P. (1997) Nat. Struct. Biol. 4, 801–804.
[18] Yao, J., Chung, J., Eliezer, D., Wright, P.E. and Dyson, H.J. (2001) Biochemistry 40, 3561–3571.
[19] Dyson, J. and Wright, P.E. (2001) Methods Enzymol. 339, 258–270.
[20] Kohl, N.E., Emini, E.A., Schleif, W.A., Davis, L.J., Heimbach, J.C., Dixon, R.A., Scolnick, E.M. and Sigal, I.S. (1988) Proc. Natl. Acad. Sci. USA 85, 4686–4690.
[21] Davies, D.R. (1990) Annu. Rev. Biophys. Biophys. Chem. 19, 189–215.
[22] Yamazaki, T., Nicholson, L.K., Torchia, D.A., Stahl, S.J., Kaufman, J.D., Wingfield, P.T., Domaille, P.J. and Campbell-Burk, S. (1994) Eur. J. Biochem. 219, 707–712.
[23] Freedberg, D.I., Wang, Y., Stahl, S.J., Kaufman, J.D., Wingfield, P.T., Kiso, Y. and Torchia, D.A. (1998) J. Am. Chem. Soc. 120, 7916–7923.
[24] Ishima, R., Wingfield, P.T., Stahl, S.J., Kaufman, J.D. and Torchia, D.A. (1998) J. Am. Chem. Soc. 120, 10534–10542.
[25] Ishima, R., Freedberg, D.I., Wang, Y., Louis, J.M. and Torchia, D.A. (1999) Structure 7, 1047–1055.
[26] Panchal, S.C., Pillai, B., Hosur, M.V. and Hosur, R.V. (2000) Curr. Sci. 79, 1684–1695.
[27] Cheng, Y.E., Yin, F.H., Foundling, S., Blomstrom, D. and Kettner, C.A. (1990) Proc. Natl. Acad. Sci. USA 87, 9660–9664.
[28] Dilanni, C.L., Davis, L.J., Holloway, M.K., Herber, W.K., Darke, P.L., Kohl, N.E. and Dixon, R.A.F. (1990) J. Biol. Chem. 265, 17348–17354.
[29] Panchal, S.C., Bhavesh, N.S. and Hosur, R.V. (2001) J. Biomol. NMR 20, 135–147.
[30] Kay, L.E., Ikura, M., Tschudin, R. and Bax, A. (1990) J. Magn. Reson. 89, 496–514.
[31] Grzseik, S. and Bax, A. (1992) J. Magn. Reson. 96, 432–440.
[32] Grzseik, S. and Bax, A. (1992) J. Magn. Reson. 99, 201–207.
[33] Grzseik, S. and Bax, A. (1992) J. Am. Chem. Soc. 114, 6291–6293.
[34] Pervushin, K., Riek, R., Wider, G. and Wüthrich, K. (1997) Proc. Natl. Acad. Sci. USA 94, 12366–12371.
[35] Wishart, D.S., Sykes, B.D. and Richards, F.M. (1991) J. Mol. Biol. 222, 311–333.
[36] Spera, S. and Bax, A. (1991) J. Am. Chem. Soc. 113, 5490–5492.
[37] Wishart, D.S. and Sykes, B.D. (1994) Methods Enzymol. 239, 363–392.
[38] Wishart, D.S. and Sykes, B.D. (1994) J. Biomol. NMR 4, 171–180.
[39] Wishart, D.S., Bigam, C.G., Holm, A., Hodges, R.S. and Sykes, B.D. (1995) J. Biomol. NMR 5, 67–81.
[40] Schwarzinger, S., Kroon, G.J.A., Foss, T.R., Wright, P.E. and Dyson, H.J. (2000) J. Biomol. NMR 18, 43–48.
[41] Schwarzinger, S., Kroon, G.J.A., Foss, T.R., Chung, J., Wright, P.E. and Dyson, H.J. (2001) J. Am. Chem. Soc. 123, 2970–2978.
[42] Vuister, G.W. and Bax, A. (1993) J. Am. Chem. Soc. 115, 7772–7777.
[43] Montelione, G., Winkler, M.E., Rauenbuehler, P. and Wagner, G. (1989) J. Magn. Reson. 82, 198–204.
[44] Pillai, B., Kannan, K.K. and Hosur, M.V. (2001) Proteins 43, 57–64.
[45] Chan, H.S. and Dill, K.A. (1997) Nat. Struct. Biol. 4, 10–19.
[46] Dobson, C.M. and Karplus, M. (1999) Curr. Opin. Struct. Biol. 9, 92–101.
[47] Brockwell, D.J., Smith, D.A. and Radford, S.E. (2000) Curr. Opin. Struct. Biol. 10, 16–25.
[48] Plaxco, K.W., Morton, C.J., Grimshaw, S.B., Jones, J.A., Pitkeathly, M., Campbell, I.D. and Dobson, C.M. (1997) J. Biomol. NMR 10, 221–230.